ADVANCED HEALTHCARE MATERIALS
www.advhealthmat.de

Polymer Bioelectronics: A Solution for Both Stimulating and Recording Electrodes

*Estelle A. Cuttaz, Zachary K. Bailey, Christopher A. R. Chapman, Josef A. Goding, and Rylie A. Green**

The advent of closed-loop bionics has created a demand for electrode materials that are ideal for both stimulating and recording applications. The growing complexity and diminishing size of implantable devices for neural interfaces have moved beyond what can be achieved with conventional metallic electrode materials. Polymeric electrode materials are a recent development based on polymer composites of organic conductors such as conductive polymers. These materials present exciting new opportunities in the design and fabrication of next-generation electrode arrays which can overcome the electrochemical and mechanical limitations of conventional electrode materials. This review will examine the recent developments in polymeric electrode materials, their application as stimulating and recording electrodes in bionic devices, and their impact on the development of soft, conformal, and high-density neural interfaces.

1. Introduction

Recent advances at the nexus of bioelectronic materials, mechatronics, and electrical engineering have driven the development of a new generation of fully integrated bionic implants as therapeutic and rehabilitative technologies. This has enabled spinal cord stimulation to restore patient mobility,[1] sensory feedback to improve dexterity in prosthetic limb control,[2] and brain-machine interfacing to decode speech directly from the cortex,[3] as seen in **Figure 1**. Critical to these technologies is the communication between the synthetic device and the biological tissue. There is an inherent complexity in forming a robust chronic closed-loop interface due to the different ideal criteria for recording and stimulation with implanted electrodes. Recording interfaces require low electrode-tissue impedance for efficient neural recording with a high signal-to-noise ratio (SNR), whereas stimulating electrodes require high charge injection capacity for safe, reversible, and efficient stimulation.[4] Both stimulating and recording electrodes also require consideration of biocompatibility, mechanical stiffness, and long-term physicochemical and mechanical stability. These requirements directly inform the materials that can be used for these interfaces. Metals such as platinum (Pt), platinum-iridium (PtIr), and gold (Au) are frequently used as electrode materials due to their high conductivity and biological inertness. Although these metals have been used successfully for individual application of recording or stimulation, achieving stable chronic closed-loop functionality has remained difficult due to limitations from the materials themselves.[5]

For metallic electrodes, these limitations are characterized by high electrode impedance caused by low electrochemical surface area (ESA), and poor charge transfer caused by the material itself. As the geometrical area of flat electrodes is reduced to improve recording resolution, the ESA is reduced causing high interfacial impedance due to a reduction in double-layer capacitance.[6] A common material strategy to overcome these limitations on flat electrode surfaces is to confer higher ESA via the application of nano- or micro-structured surface features.[7,8] The increased ESA from surface modification provides additional interfacial area for charge accumulation on the electrode surface, thus reducing impedance and improving SNR.

One of the most challenging limitations for metallic electrodes is their capacity to inject charge in a safe manner. The charge transfer mechanism of an electrode is a property of the material itself and can occur via faradaic or non-faradaic (capacitive) mechanisms as shown on **Figure 2**.[4,6,9–10]

Faradaic charge transport involves the transfer of electrons at the electrode-electrolyte interface via surface-confined reduction and oxidation, whereas capacitive charge transfer utilizes accumulated charged chemical species at the electrode/electrolyte interface by charging and discharging the electrical double layer formed at the material surface. The majority of metals transfer charge via faradaic charge transfer where the material participates in the electron transport. This transfer of

E. A. Cuttaz, Z. K. Bailey, C. A. R. Chapman, J. A. Goding, R. A. Green
Department of Bioengineering
Imperial College London
London SW7 2BX, UK
E-mail: rylie.green@imperial.ac.uk
C. A. R. Chapman
School of Engineering and Materials Science
Queen Mary University of London
London E1 4NS, UK

The ORCID identification number(s) for the author(s) of this article can be found under https://doi.org/10.1002/adhm.202304447

DOI: 10.1002/adhm.202304447

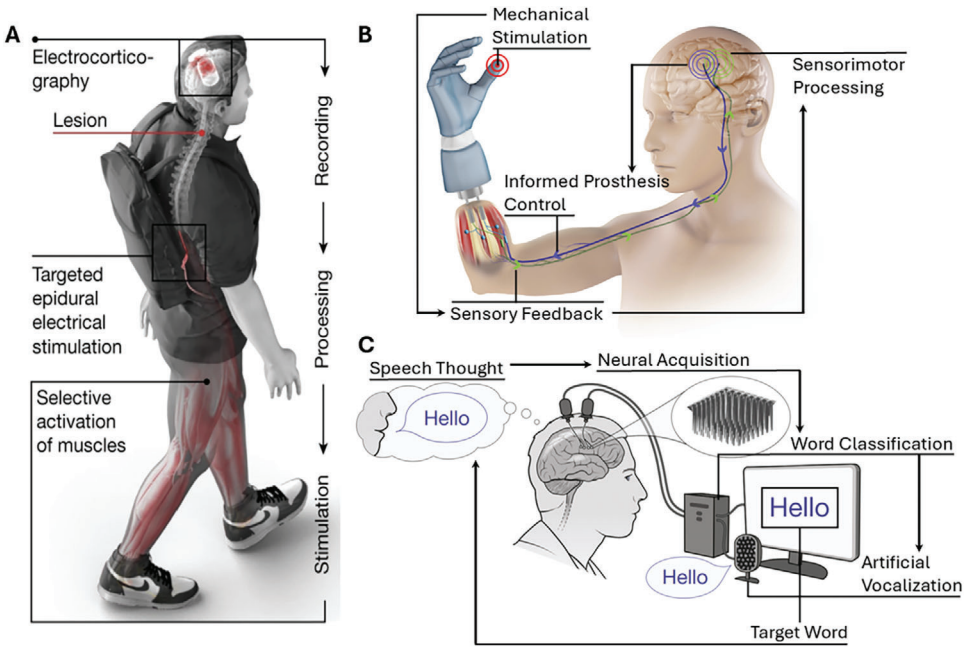

Figure 1. Recent applications of neural interfacing technologies. A) Mobility is restored in a paralyzed patient via spinal cord stimulation controlled by decoded recordings from an implanted EEG. B) Improved motor control of a prosthetic arm via sensory feedback from sensor pads in the prosthesis. C) Artificially recreated speech from decoded neural signals in the temporal lobe. (A) Reproduced with permission.[1] Copyright 2023, Springer Nature. B) Adapted with permission.[2] Copyright 2023, AAAS. (C) Adapted with permission.[3] Copyright 2023, Springer Nature.

electrons can result in the production of harmful chemical species through water electrolysis or metal electrode dissolution or corrosion, which ultimately damages both the electrode and nearby tissue.[4] Electrodes using only capacitive charge transfer benefit from improved stability; however, the purely capacitive interfaces suffer from significant limitations on the amount of charge that can be injected.

Another key limitation of metallic electrodes is their mechanical stiffness. Metals electrodes will have a stiffness in the 10′s to 100′s of GPa, significantly stiffer than the surrounding neural tissue which typically have a stiffness of 100 Pa to 10KPa. Following implantation of stiff metal electrodes, the inflammatory response due to implant injury is continually upregulated by this mechanical mismatch. This prolonged response allows

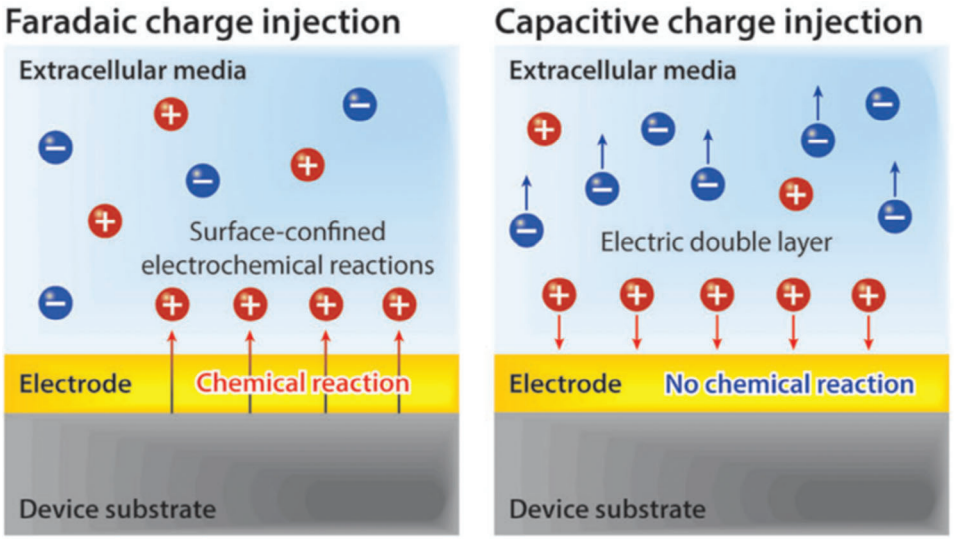

Figure 2. Schematics of faradaic (left) and capacitive (non-Faradaic) (right) charge injection processes. Faradaic charge injection mechanism relies on the transfer of electrons through surface-confined electrochemical reactions at the electrode-electrolyte interface. Capacitive charge injection includes the charging/discharging of the electric double layer by accumulation of ions at the electrode material interface without electrochemical reactions. Reproduced with permission.[10] Copyright 2018, Royal Society of Chemistry.

inflammatory-mediating cells (macrophages, microglia, astrocytes) to isolate the implant in fibrotic scar tissue, increasing the distance between the implant and the target neural tissue. Additionally, fibroblasts and extracellular matrix proteins present in fibrotic encapsulation decrease ion mobility between the neural tissue and the implanted electrodes. This chronic response to an implant, results in higher impedance for stimulating electrodes and reduced SNR for recording electrodes. The foreign body reaction incited by this stiffness mismatch has been described in mechanistic detail by Gilmour et al.[11] This mechanical mismatch can be reduced by using softer materials as coatings on metal electrodes or through the more recent developments of fully polymeric electrodes, which is further discussed in Sections 3 and 4.

Many metallic surface modifications have been investigated to improve both ESA and charge transfer mechanisms. These include the coating of the electrode surface with porous iridium oxide (IrOx) or titanium nitride (TiN). These metal compounds have the ability to transfer electrons and ions efficiently, as they possess high charge injection capacities. However, this improvement in charge injection is reliant on the use of a potential bias to generate an interface where ions are readily available for charge transfer, and the impact of this bias on tissue response and the local environment is not fully understood.[12] Another option relies on the deposition of metallic nanostructures such as Au nanowires or Pt black nanoparticles to increase the charge transfer area.[13,14] While these highly engineered metal-based materials have had success in improving recording and stimulation functionality, they do not address any of the mechanical or biological shortcomings of metallic technologies.

Polymer-based electrode materials such as conducting polymers (CPs) have received significant attention due to their inherently superior charge transfer properties, low impedance, high charge injection limits, and high SNR. They are especially promising when operating within an ionic environment, such as implant devices, where CP ion mobility is advantageous. These unique properties of CPs enabled by mixed-mode conduction make them an ideal candidate for both stimulating and recording applications. When stimulating, electron conduction within the 3D polymer network enables capacitive charge transduction from the electronic hardware to ions required to modulate the biological environment. This process occurs throughout the entire volume of the electrode, resulting in a lower voltage on the electrodes because of vastly increased volumetric ESA. When recording, there is a direct ionic transfer from the surrounding environment into the polymer network, facilitated through the charged CP backbone, thereby avoiding the need for faradaic chemical reactions that dominate the interface of metallic electrodes when transducing ions to electrons during recording.

The advent of commercially available, highly processible CPs has led to a rapid expansion in research on CP-based materials for stimulating and recording applications. As such, these polymeric bioelectronics are not just improving the performance of stimulating and recording electrodes but are fundamentally changing the way bioelectronic devices are designed, fabricated, and implemented. This review provides an analysis of the properties of CPs which make them interesting for bioelectronic applications (Section 2), their application as a coating technology (Section 3), the design of CP-based composites (Section 4), the fabrication of CP-based bioelectronic devices (Section 5), and the application of polymer bioelectronics in closed-loop applications (Section 6).

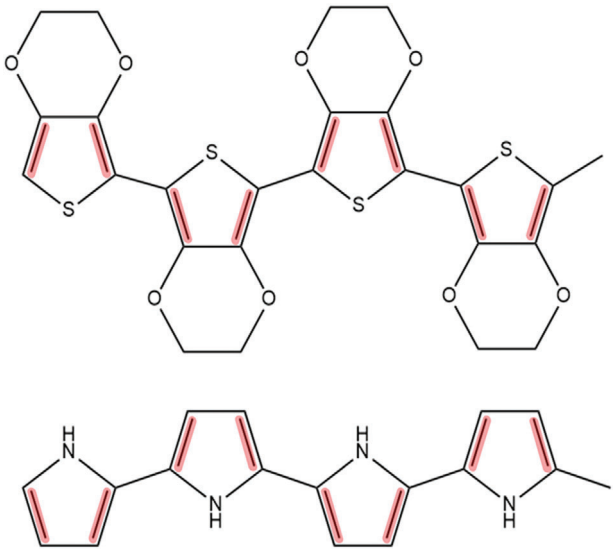

Figure 3. Chemical structures of commonly used conducting polymers including poly(3,4-ethylene dioxythiophene) (PEDOT) (top) and polypyrrole (PPy) (bottom). Red zone highlights the pi-bonds allowing easier delocalization of the electrons along the polymer backbone.

2. Conducting Polymer Properties

Conducting polymers consist of a backbone with repeating conjugated units, having an alternating double and single bond structure.[15–17] This single and double bond arrangement possesses a strong and localized sigma-bond. The double bonds also have a weakly localized pi-bond as illustrated in **Figure 3**. Due to the conjugated structure of these polymers, the p_z-orbitals in the chain of pi-bonds laterally overlap and hybridize, enabling the electrons in the pi-bonds to be delocalized thus creating a conductive pathway along the polymer backbone (intrachain) and across adjacent polymer chains (interchain). While this conjugated structure provides the ability for charge transport within and between polymer chains, the high structural and morphological disorder from the polymerization of CPs greatly limits pi-bond delocalization ultimately hindering efficient charge conduction. Therefore, another key element, known as a dopant molecule, is typically required to confer higher conductivity. The addition of a dopant enables the incorporation of external charge carriers into the polymer in the form of polarons, bipolarons or solitons that cause local distortions in the CP structure.[15] Through the introduction of these charge carriers, doping increases the free charge carrier density, enabling the movement of charge along the backbone, and enhancing electronic conductivity.

Unlike metallic electrodes, organic CP electrodes are not strictly limited to charge conductance via double-layer capacitance (see **Figure 4** for comparison). Organic polymer electrodes exhibit a property called volumetric capacitance (denoted as C*) that relies on the porosity of the polymer network and ion

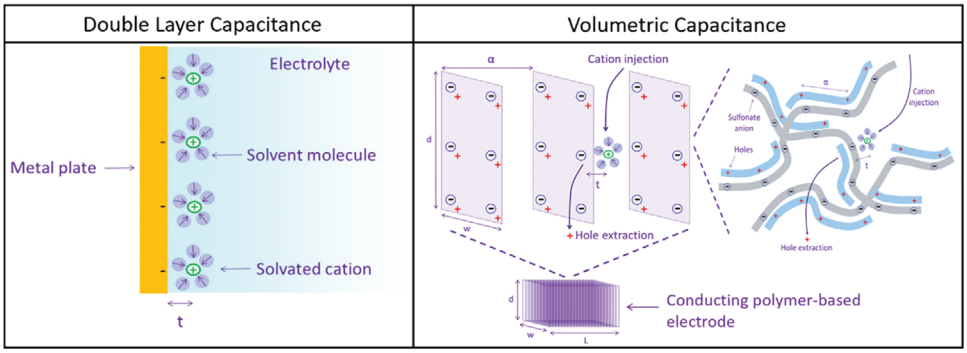

Figure 4. Schematics showing the difference in charge transfer mechanisms between double-layer capacitance in metal-based electrodes and volumetric capacitance in CP-based electrode. Adapted with permission.[20] Copyright 2016, Wiley Periodicals, Inc.

mobility (μ) throughout the entire volume of the polymer electrode. There has been a convergence in this research field on a particular electrochemical metric C*μ (pronounced "C star mu") as a value to optimize in organic polymer electrode development. This metric is representative of total charge transfer through this mixed mode conduction (ionic and electronic).[18] This method of conduction eliminates the reliance on double-layer capacitance and strict surface area for organic polymer electrodes, so electrodes coated in poly(3,4-ethylene dioxythiophene complexed to polystyrene sulfonate (PEDOT:PSS) have been manufactured down to 10 μm in diameter while still maintaining a sufficient SNR for recording signals from individual neurons.[19]

While early research into biomedical applications for CPs focused on a variety of polymer chemistries (see **Table 1**) including polythiophenes, polypyrrole, polyaniline, the advent of commercially available formulations of PEDOT:PSS has seen a large shift in focus toward PEDOT-based bioelectronics. A review of publication titles using Scopus shows the percentage of publications using "PEDOT:PSS" versus "Conducting(/ive) Polymers" has risen from 0% in the year 2000, to over 50% in the year 2020. The main reasons for this shift includes the ease of use & processability of PEDOT:PSS, its electrical and physicochemical stability, and its relatively high conductivity.

3. Conducting Polymer Coatings

Depositing CP layers onto conventional, planar metal electrodes, results in an interface with lower impedance by taking advantage of the volumetric capacitance of the deposited layer. One excellent example of this is the development of "Neurogrid", an ultrathin surface electrode array with a thickness of 4 μm, using microfabricated PEDOT:PSS-coated Au electrodes with a contact area of 10 μm × 10 μm as shown on **Figure 5**.[19] In this application the PEDOT:PSS coating enabled the recording electrode sites to be miniaturized past what would be conventionally possible with Au alone. Due to its ultra-conformability and high electrode density matching the spatial scale of neurons, the Neurogrid was able to record both local field potentials (LFPs) and action potentials from superficial cortical layers of both rodents and epilepsy patients, without the need for tissue penetration. An SNR of 45 dB at a frequency of 10 Hz was reported for surface recording acquired by the Neurogrid. This was noted to be significantly higher than that of a penetrative depth recording obtained by a silicon probe which was measured at 38 dB. Recently, optimization of the electronic connection, packaging, and placement of the Neurogrid array has improved the yield and quality of the recordings and resulted in the measurement of single-unit activity from the cortical surface of the human brain intraoperatively.[22]

Table 1. Chemical formulas and conductivity values of CPs commonly used for biomedical applications. Adapted with permission.[21] Copyright 2018, American Chemical Society.

Polymer	Formula	Conductivity [S cm^{-1}]
Polyacetylene	$[C_2H_2]_n$	10^5
Polypyrrole	$[C_4H_2NH]_n$	10^0–10^2
Polyaniline	$[C_6H_4NH]_n$	10^{-2}–10^0
Polythiophene	$[C4H_4S]_n$	10^0–10^3

A similar approach was investigated by Ganji et al., where flexible PEDOT:PSS based surface microarrays were fabricated for ECoG monitoring.[23] The PEDOT-coated electrodes had a more uniform and order of magnitude lower impedance when compared to that of Pt electrodes of equivalent geometry. These arrays could not record at a single neuron resolution, presumably due to its larger 50 μm diameter electrode area and limited device surface contact to the brain surface. However, they were able to record an evoked cognitive response to audio-visual stimuli from human subjects. The PEDOT coated device exhibited a higher difference in power of 6.2 dB in the 10–50 Hz band between baseline and epileptiform activity compared to a difference of 2.4 dB measured with the clinical metallic electrodes, suggesting the potential of polymeric coating to facilitate recording at higher SNR. Additional human studies were conducted using high-density PEDOT:PSS based surface arrays to record patients undergoing surgical resection of cortical tissue in the case of tumor or epilepsy.[24] The PEDOT:PSS arrays demonstrated similar cortical recording to current clinical metal electrodes but were able to detect other types of activity such as unitary events and slower oscillatory events.

The mixed conduction mode of CPs combined with their high current injection capacity is of particular interest for efficient neural stimulation without breaching electrochemical safety. CP-coated metal microelectrodes have been shown to outperform metal technologies in stimulation applications across both in vitro and in vivo settings.[25] CP coatings assessed in vitro were

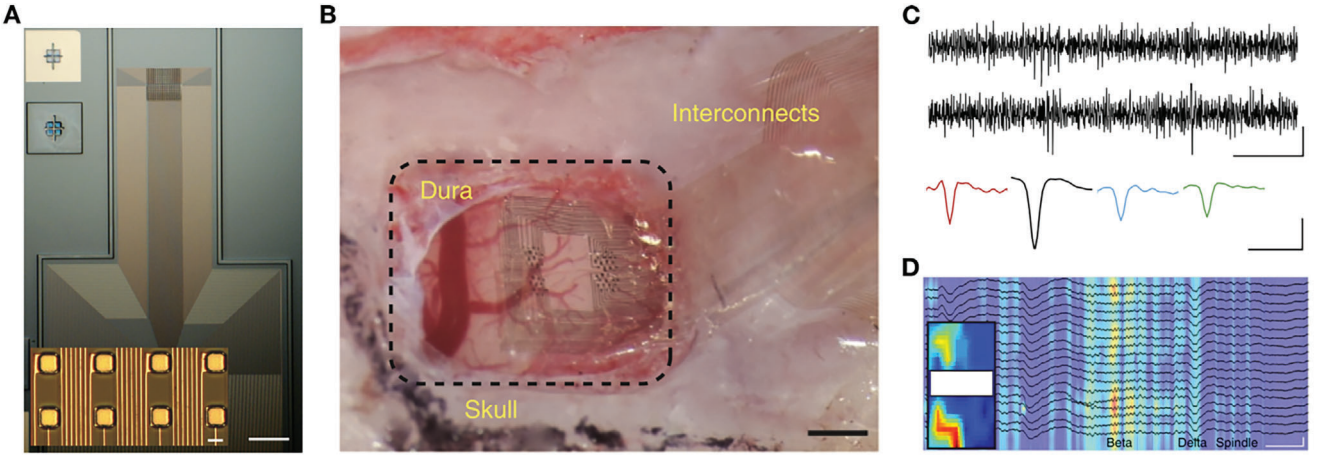

Figure 5. NeuroGrid structure and intraoperative recordings of LFP and spikes in epilepsy patients. A) Optical micrograph of a 256-channel NeuroGrid (scale bar = 1 mm). Inset shows the PEDOT:PSS-coated Au recording sites with an electrode surface area of 10 × 10 μm^2 and an interelectrode spacing of 30 μm (scale bar = 10 μm). B) Due to its ultrathin architecture, the Neurogrid conforms to the surface of the rat somatosensory cortex following dura mater removal (scale bar = 1 mm). C) High-pass-filtered traces of intraoperative NeuroGrid recordings in epilepsy patients showing spiking activity (scale bars = 20 ms × 40 μV) (top) and sample spike waveforms acquired from different recording sites (scale bars = 1 ms × 40 μV) (bottom). D) Recordings measured intraoperatively in patients undergoing epilepsy surgery showing sample multichannel local field potentials (LFPs) (black traces) overlaid on time-frequency spectrogram filtered at beta frequency (18–25 Hz). Inset shows areas with high beta-frequency power detected at spatially coherent clusters of activity on the NeuroGrid (scale bars = 500 ms × 750 μV). Reproduced with permission.[19] Copyright 2014, Springer Nature.

able to inject ≈3 mC cm^{-2} while retaining the residual voltage within the electrochemical safety limits of the water window. This is 15 × more charge when compared to PtIr and IrOx-coated electrodes. Similarly, CP coatings demonstrate significantly reduced voltage transients upon biphasic current stimulation over an implantation period of two weeks in rat cortex compared to PtIr controls. A report from Green et al.[26] demonstrated the stimulation abilities of CPs across both in vitro and acute in vivo studies. In vitro evaluation showed that PEDOT-coated electrode arrays had charge injection limits within the range 1.5–2.6 mC cm^{-2}, which is 15 to 35 times higher than that of Pt electrodes ranging from 0.05–0.07 mC cm^{-2}. Once implanted in the suprachoroidal space of the eye, PEDOT electrodes demonstrated lower voltage transients and were able to elicit neural responses at lower charge injection levels compared to Pt controls.

This mode of charge transfer also shows promise in enabling stimulation over a lower frequency range than is possible with conventional metallic electrodes. Stimulation at DC and low-frequency regimes have been suggested as one approach to treat chronic disorders through blocking and modulation of unmyelinated fibers for pain therapy, vagus nerve stimulation (VNS) or hypertension treatment.[27] Alternatively, applications in cognitive enhancement through nerve blocking or stimulation with direct and alternative current has been reported.[27–31] Metals cannot safely inject charge at very low frequencies and DC without triggering electrochemical reactions such as corrosion and electrolysis. This increases the risk of device failure as well as damage to the surrounding tissues due the release of harmful byproducts.[27,28,32] In contrast, CPs can safely deliver charge at these frequencies without undergoing detrimental or irreversible chemical reactions.[27,32,33] For example, PEDOT-coated nerve cuff electrodes were able to deliver low-frequency alternating current blocking waveforms to reversibly block VNS-induced bradycardic effect in rats.[31]

CP coatings also have the advantage of being one to two orders of magnitude less stiff than metals typically used as electrodes. As seen in **Figure 6**, while CPs are still significantly stiffer than neural tissue, they reduce the strain mismatch at the neural interface, which can help to reduce the inflammatory response upon implantation.

While providing improved functionality over bare metal electrodes, CP coatings have not seen wide uptake, as they possess brittle mechanics and can be prone to delamination during electrical stimulation.[35–37] One strategy to impart mechanical compliance and durability to these organic conductors is to incorporate them into softer polymeric matrices, such as hydrogels or elastomers to produce conductive hydrogels (CHs) or conductive elastomers (CEs).[12,38] The resulting composites combine both the electrochemical performance of the organic conductors with the mechanical stability of the secondary polymer matrix. The addition of this secondary polymer network has also been suggested to facilitate a wider range of processing and manufacturing techniques for an otherwise limited scope of CP fabrication approaches.[39]

4. Conducting Polymer Composites

Polymer macrostructures can generally be subdivided into three classifications that are correlated to mechanical integrity: thermosets, thermoplastics, and elastomers (see **Figure 7**). Thermosets are the most robust and rigid networks with high degrees of covalent bonding. They are normally insoluble in most solvents and not processable once set. Thermoplastics are typically non-covalently linked polymer-based materials with dense polymer strand networks. Despite the lack of covalent bonding, these materials share similar structural properties as thermosets unless under heat when they can be reshaped as a viscoelastic material. Elastomers have less crystallinity compared to

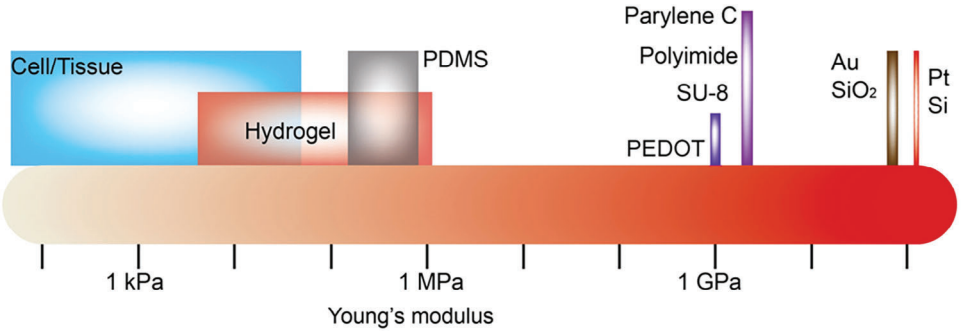

Figure 6. Typical values of Young's modulus for neural tissue and materials commonly used in neural interfaces. Reproduced with permission.[34] Copyright 2020, Wiley.

thermoplastics because of a larger amount of branching and cross-linking. They maintain their structural integrity through mechanically interlocked strands that have been entangled during the polymerization process. The interlocking strands act as molecular springs that allow the material to stretch before structural damage occurs and return to its original structure due to the entropic conformational gain in the stretched strands. Gels (commonly called hydrogels) are similarly structured to elastomers except even more amorphous, leaving larger gaps in between polymer strands, leading to the swelling property of gels, which can be utilized to load or capture biomolecules or other drugs.

Since the late 1950s, thermoset epoxy resins and polyurethanes have been used for encapsulation in the development of implantable electrophysiological devices, such as the pacemaker and early neural stimulators.[41] However, with the introduction of CPs and swelling hydrogels, entire electrode arrays (insulation, electrode, interconnecting tracks, and tissue interface) can be manufactured from soft, flexible polymeric materials, including recently developed nerve cuff electrode arrays.[42] Fully polymeric electrode arrays utilize an interpenetrating polymer network (IPN) for the CP electrode, which consists of two or more polymers in a single network mesh, typically capitalizing on the intrinsic properties of both individual polymer networks. Incorporating CPs into composite structures not only improves the mechanical stability of the interfaces, but also confers flexibility to the electrode surfaces themselves. This flexibility enables a high degree of conformability as well as reduced mechanical mismatch with soft target tissue. Enhanced conformability increases the amount of direct surface contact between the charge-exchanging electrode surface and the electro-sensitive target tissue, which lowers electrical impedance as there is less fluid ingress in the electrode-tissue interface.[43] The lower mechanical mismatch can also decrease electrical impedance by lowering the scar tissue development in the post-implantation foreign body response (FBR).[44]

One further benefit of developing composite materials for electrode surfaces is the potential to increase the conductance of charge through the volume of an organic polymer electrode by diffusion of water into the nanopores of the polymer network. Mechanically, this diffusion of water will result in swelling if the polymer network is penetrable, which will increase the ion mobility throughout the volume. This process of water swelling is vital in the production of hydrogels, in which multiple semi-interpenetrating polymer networks (SIPN) mesh together to lock in water along the polymer backbone. **Figure 8** demonstrates the chemical and mechanical tunability of complex polymer networks.[45] A polyethylene glycol (PEG)-based bioactive hydrogel has been demonstrated to mimic the extracellular matrix (ECM) with biomolecules to improve tissue adherence and ingrowth following implantation. Additionally, IPNs and SIPNs

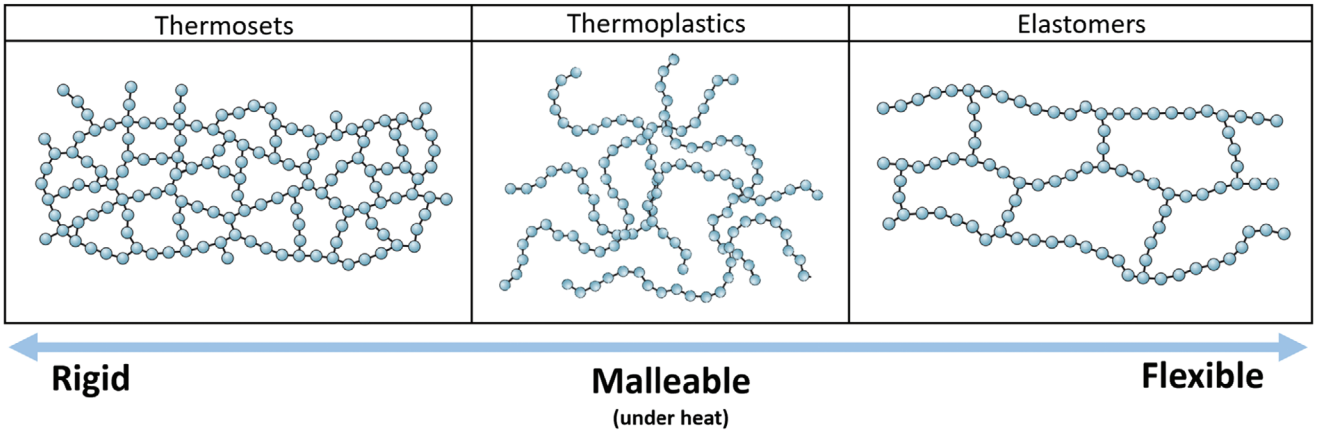

Figure 7. Supramolecular representation of most common polymer network structures. Reproduced with permission.[40] Copyright 2019, Wiley.

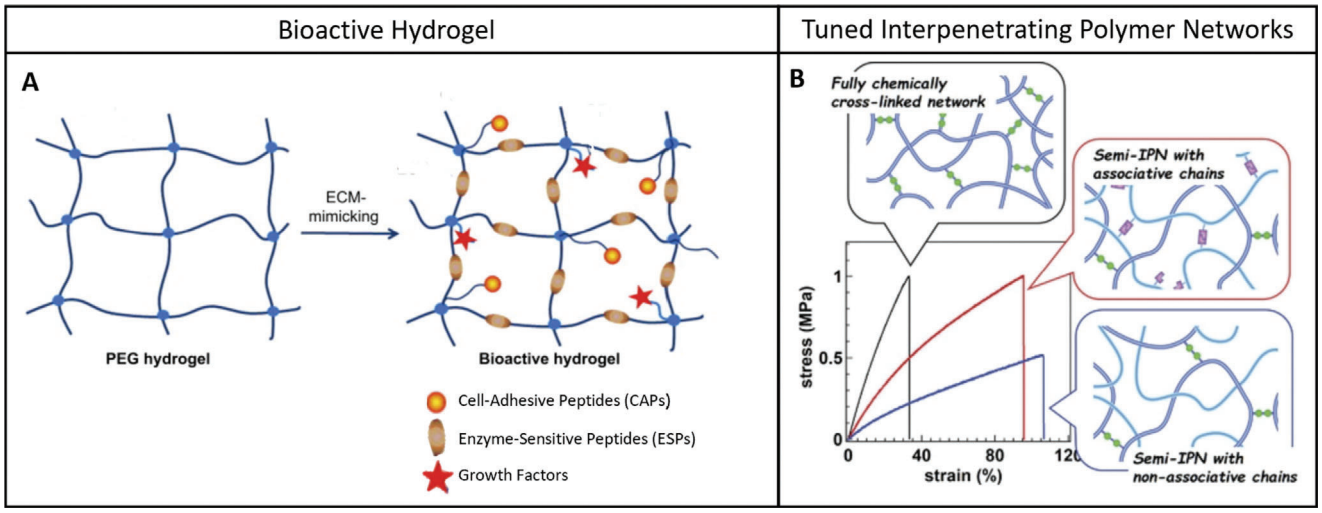

Figure 8. Two examples of more recent advancements in polymer network development to increase bioactivity and tunability of mechanical properties. A) A PEG-based hydrogel has been loaded with cell-adhesive peptides (CAPs), enzyme-sensitive peptides (ESPs), and Growth Factors to recreate the extracellular matrix (ECM) environment for a higher degree of integration with organic tissue. B) The stress-strain relationship is compared across three mechanically tuned polymer networks. A fully cross-linked interpenetrating polymer network (IPN) can withstand higher stress, but it cannot stretch much before failure. A semi-interpenetrating polymer network with non-associative chains can stretch the furthest before failure but can only withstand a lower degree of stress. A semi-interpenetrating polymer network with associative chains can both withstand higher stresses and stretch further without failure. (A) Reproduced with permission.[45] Copyright 2019, Wiley. (B) Reproduced with permission.[46] Copyright 2017, Springer Nature.

can be combined with associative chains to further control cross-linking and tune the mechanical properties of the hydrogel to match underlying tissue.

4.1. Conductive Hydrogels

Similar to CP films, CHs have been widely investigated as a coating technology. However, they were shown to achieve significantly improved electrochemical performance compared to bare metal electrodes.[47,48] The swelling property of the hydrogel component offers additional access to the CP network, which can be leveraged for charge transfer in the form of ions, greatly expanding the amount of charge that can be transduced with surrounding tissues without triggering harmful redox reactions. Additionally, since hydrogels typically have a stiffness in kPa range and viscoelastic properties similar to that of soft tissue, they can further reduce the mechanical mismatch at the neural interface (refer to Figure 6). Precurled and planar metallic electrode arrays coated with CHs were shown to significantly improve the in vitro charge transfer properties of nerve cuff arrays and provide stable long-term delivery of high-frequency neural blocking waveforms.[49] Specifically, CH-coated devices had charge injection limits ranging from 13 to 15 μC cm^{-2}, significantly higher than that of the bare metallic electrode controls measured at 2 to 4 μC cm^{-2}. Similar CH electrode technologies implanted in rats over a 5-week period were found to be stable following chronic stimulation, with the benefit of higher charge storage and injection capacities compared to metallic controls as depicted on **Figure 9**.[37] The addition of ionic liquid additives to the preparation of CHs has resulted in a material system with even higher level of conductivity, and have been shown to be processable into soft and elastic electrode arrays.[50] Compared to equivalent Pt devices, CH-based electrode arrays have demonstrated improved electrochemical performance and in mice sciatic nerve have been shown to deliver localized stimulation of muscle movements at low voltage.

4.2. Conductive Elastomers

CEs combining CPs and elastomeric matrices have resulted in the formulation of compliant and conductive composite materials, specifically suitable for applications in flexible bioelectronic devices. Guo et al.[51] reported the fabrication of a fully polymeric device using a composite film of the CP polypyrrole and polycaprolactone-block-polytetrahydrofuran-block-polycaprolactone (PCTC) as electrode and track materials. The resulting stretchable multielectrode array was found to be able to acutely record EMG.[51] A similar approach has been developed from composites of PEDOT:PSS and polyurethane elastomers (PU). A flexible peripheral nerve cuff electrode array was prepared using the PEDOT:PSS/PU composite as the sole conductor and PDMS as the insulation material. Ex vivo studies using a rat sciatic nerve model have shown that the polymeric cuff CE devices were functionally equivalent to PtIr devices of similar format, with the benefit of significantly larger charge injection limits.[42] All cuff CE devices have been reported to have charge injection limits ranging from 0.44 – 3.13 μC ph^{-1}, which is approximately a 1.8 to seven-fold increase compared to the PtIr devices (which varied ≈0.11 – 0.45 μC ph^{-1}).

While CP composites have been shown to maintain the high electroactivity of CPs, different strategies have been investigated to further improve the mechanical properties of the material

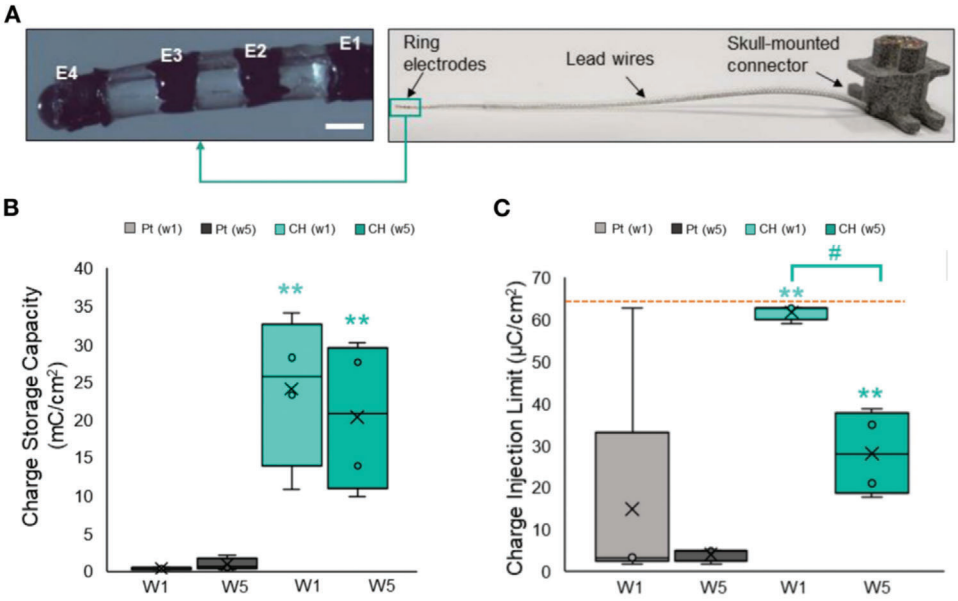

Figure 9. Electrochemical performance of a CH-coated cochlear implant electrode array recorded in vivo over a period of 5 weeks. A) Pictures showing the electrode array with four CH-coated Pt ring electrodes located at the tip of the implant. Each ring electrode is connected via a leadwire assembly to a skull-mounted percutaneous connector (scale bar = 0.3 mm). B) Charge storage capacities and (C) charge injection limits of CH-coated and bare Pt electrodes measured in vivo at week 1 and week 5 post implantation.© IOP Publishing. Reproduced with permission.[37] Copyright 2020, IOP Publishing Ltd.

composite to ensure stable performance when implanted within dynamic, motile tissues. CP composite electrodes for epidermal biopotential monitoring were produced from PEDOT:PSS and waterborne PU with the addition of the additive and plasticizer D-sorbitol to improve material stretchability.[52] The resulting dry electrodes combined high conductivity up to 545 S cm^{-1} and stretchability with an elongation at failure of 43%, ideal for on-skin applications. High-quality encephalogram (EEG) signals were also recorded. While additives can pose a risk of leaching and damage both the surrounding tissues and material properties, an alternative way to impart stretchability to CP composites has been reported. Kayser et al.[53] synthesized block copolymer of PEDOT:PSS-b-poly(poly(ethylene glycol) methyl ether acrylate) (PPEGMEA) using a reversible addition–fragmentation chain transfer (RAFT) polymerization. The intrinsically stretchable PEDOT:PSS-b-PPEGMEA material exhibited low Young's modulus in the MPa range and with a conductivity level at 14.8 S cm^{-1}.

The addition of carbon nanotubes (CNTs) to CP composites has been suggested as an approach to improve composite durability due to the toughness of CNTs. Zheng et al.[54] proposed the fabrication of fully polymeric and elastomeric composite wires via extrusion of a blend of polyethylene glycol (PEG)-PEDOT copolymer, CNTs, and polydimethylsiloxane (PDMS). The resulting wire had a low Young's modulus of 500 to 1000 kPa and a conductivity ranging from 1.5 to 5 S cm^{-1}. **Figure 10** shows that compared to stainless steel technologies of similar geometric surface area, the soft PEDOT-PEG/CNT wire was able to electrically stimulate muscles with lower current stimulation thresholds after 4 weeks of implantation and displayed reduced inflammation after 3 months of implantation.[55]

5. Fabrication and Processing Considerations

The transition from using purely rigid, metallic conductors to an incorporation of soft, organic, polymer-based conductors has increased the applicability of bioelectronic devices by widening the design space for bioengineers. However, this design space is practically limited by the methods required to fabricate solid electrodes from the starting material. Most of the intrinsic properties of a particular polymer that govern processibility stem from the original polymerization technique, which is heavily impacted by the amount of branch functionality and the chemistry of crosslinks.[56] However, it is also common to start with a raw polymer stock in the form of pellets, sheets, or powders. While polymer materials have enabled new manufacturing techniques for electrodes and research continues to improve and diversify these manufacturing techniques, it is important to understand the current limitations of fabrication during the design process. This section will explore the implications of using conductive polymers for electrode production on manufacturing processes and the overall electrode design for a particular application.

5.1. Manufacturing Processes

The primary characteristic of CPs that enables a greater range of manufacturability compared to that of traditional metal conductors is the lower processing temperature. In contrast to a strong atomic lattice in metals, the weaker intermolecular forces and more irregular molecular stacking due to branching typically result in much lower melting points for polymers and polymeric dispersions in solvents at normal operating temperatures without the need for heavy equipment. This ease of phase

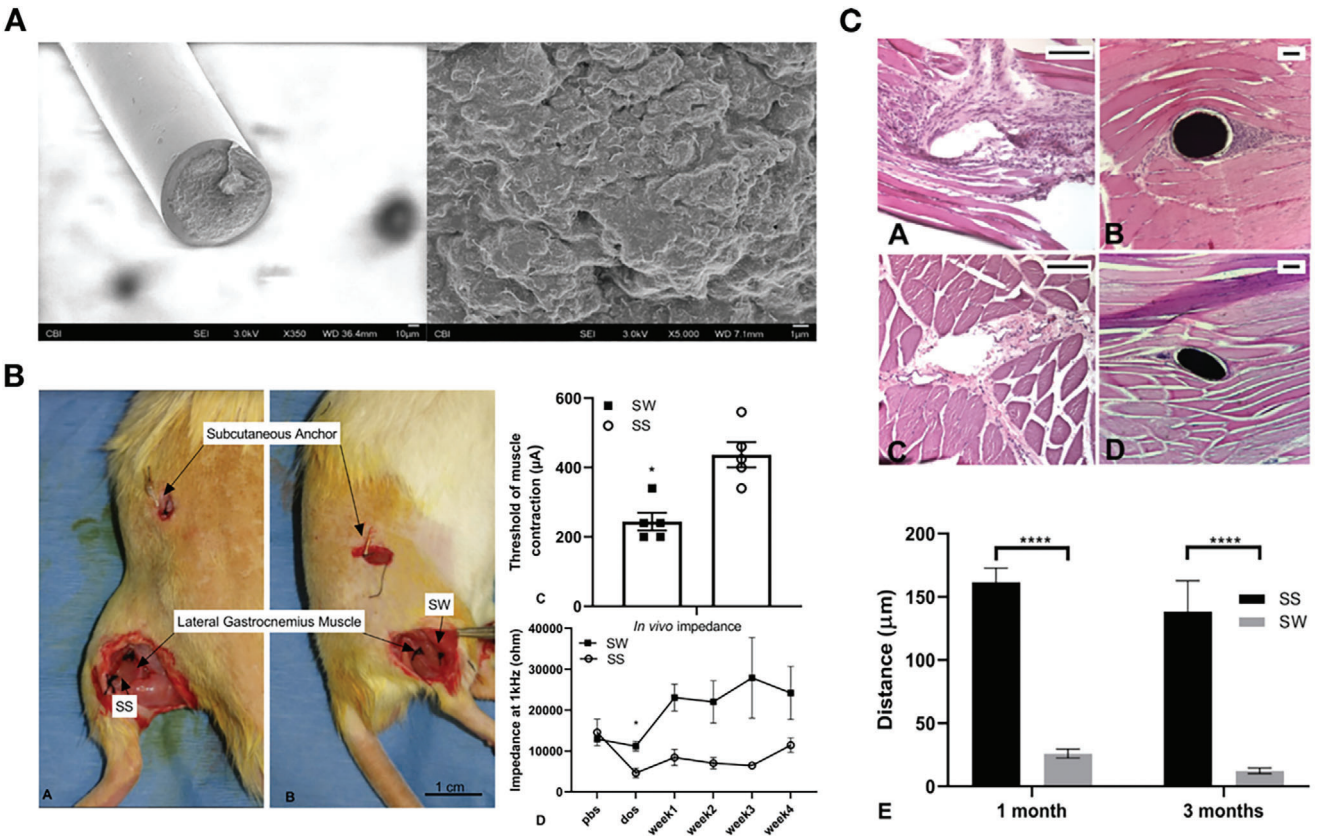

Figure 10. Conductive elastomeric wires for intramuscular stimulation. A) Scanning electron micrographs of the soft elastomeric composite wire. A cross section of the wire shows its conductive core made of a blend of polyethylene glycol (PEG)-PEDOT co-polymer, CNTs, and silicone polydimethylsiloxane and its fluorosilicone insulation(left). High magnification view of the conductive blend core can be seen (right). B) Acute in vivo implantation of a stainless-steel metal wire (SS) (a) and an elastomeric composites wire (SW) into the lateral gastrocnemius muscle for stimulation, resulting in c) lower muscle contraction thresholds and d) lower impedance over the implantation period for the polymeric wire compared to the metal SS device. C) Biocompatibility of the elastomeric wire compared to the metal SS wire. The top panel displays the haematoxylin and eosin (H&E) stains of the gastrocnemius muscle implanted with the SS (a and c) and the SW (b and d) after 1 and 3 months of implantation, respectively (Scale bars = 100 μm). Graph e) shows the distance from the electrode to healthy muscle fibres after 1 and 3 months of implantation. (A) Reproduced with permission.[54] Copyright 2019, Wiley and (B,C) Reproduced with permission.[55] Copyright 2020, Elsevier.

transitions has increased the number of electrode manufacturing techniques and their resulting form factors (3D solids, films, dispersed fibers, etc.). The two main manufacturing process groups for CPs fall under melting processes via heat application and solution processes via dispersion.

5.1.1. Heat Processes via Melting

Thermoplastics are made from dense polymer networks that can be easily made conductive by the introduction of graphene or a CP like PEDOT:PSS.[57] Therefore, traditional thermoplastic manufacturing techniques that simply reshape a heated viscoelastic material can be employed with CPs as well, such as extrusion-infused deposition modeling (FDM), 3D printing, a wide range of injection molding techniques, and vacuum forming techniques. Most of these heat-based techniques can be used in metal manufacturing as well; however, the high melting temperature (>2000 °C) of most metals common to bioelectronic applications raises the entry barrier due to equipment and expertise needed compared to thermoplastic melting points of ≈250 °C on the high end. More complex techniques incorporate a second element besides heat to shape the polymer network. One processing technique utilizing the introduction of high-pressure air is batch foaming where a heated polymer is saturated with a gaseous foaming agent inside a pressurized autoclave. After sudden depressurization of the autoclave, the now empty gas pores remain intact, and a foam is formed.[58] One of the newest melt-based techniques incorporates an electric field by applying a voltage to a molten polymer extruded from a nozzle. The applied voltage potential forces the extruded polymer to maintain a compact, linear trajectory before it is patterned onto a collector. This melt electrowriting (MEW) technique allows for the production of polymer nanofibers that can be meshed together into a scaffold or other 3D structure based on the collector construction.[59] **Figure 11** demonstrates the effect of electrical stimulation via melt electrowritten oligoEDOT scaffolds on neurite outgrowth.[60]

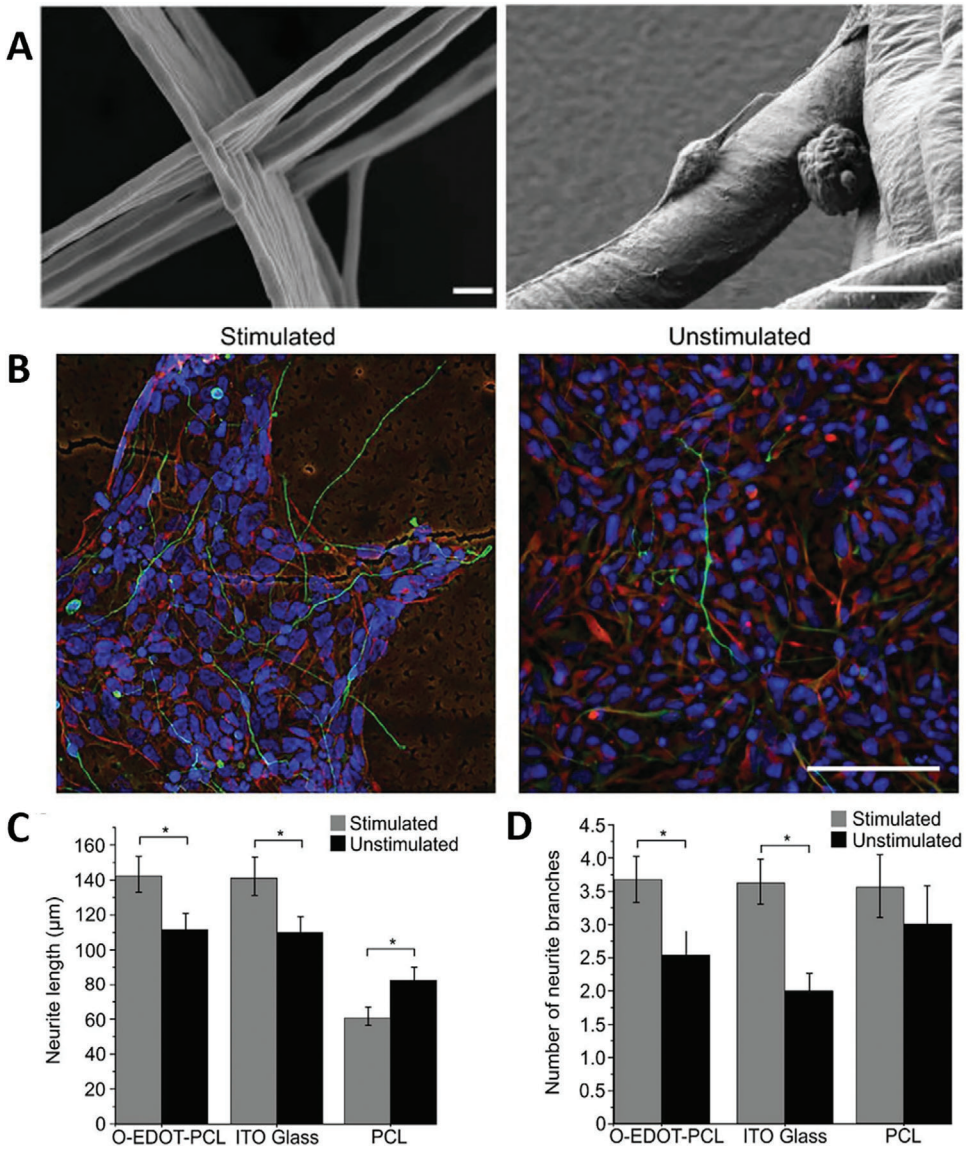

Figure 11. OligoEDOT Melt-Electrowritten Scaffold for Stimulated Neurite Growth. A) Electrowritten fibers of OligoEDOT-PCL on a glass slide (Scale bar = 20 μm) (left), neurite growth onto electrowritten fibers (Scale bar = 10 μm) (right). B) Comparison of neurite growth (βIII-tubulin, green) in electrically stimulated (left) and unstimulated (right) culture atop the electrowritten scaffolding. Comparison of C) neurite length and D) number of neurite branches in a stimulated (gray) and unstimulated (black) scaffolding. Reproduced with permission.[60] Copyright 2020, Wiley-VCH.

5.1.2. Solution Processes via Dispersion

Comparably weaker intermolecular forces within polymer networks also lead to greater dispersibility in solvents at temperatures as low as room temperature. The most common coating technique used for CPs is electropolymerization from a solution dispersion. Due to the conductive conjugated backbone of the CP monomers, it is possible to deposit polymerized material onto an electrode surface by either voltage or current application. Similarly chemical reducing agents such as iron chloride can create layers of CPs without the need for application of an electric field. Although these coatings are the easiest to deposit onto pre-patterned electrode surfaces, they suffer the worst adhesion due to weak bonding between the electrode surface and CP layer. One method to improve this is surface texturing of the underlying electrode layer. This technique has shown significant promise in improving the chronic stability of electrochemically and chemically fabricated layers of CP.[8,61] Additional coating techniques like spin coating or dip coating are typically utilized to make thin films, the thickness of which can be varied by the level of viscosity of the liquid dispersion. Thin film coating can be combined with traditional photolithographic techniques to create micro-scale features on thin film polymeric electrodes.[62] Curing mechanisms like heat or UV light can then be used to solidify these thin films. Curing mechanisms can also be used to solidify the liquid polymers into 3D shapes with FDM or stereolithographic printing using UV light for rigid solids and rapid solvent-exchange curing systems for softer colloids.[63] **Figure 12** shows

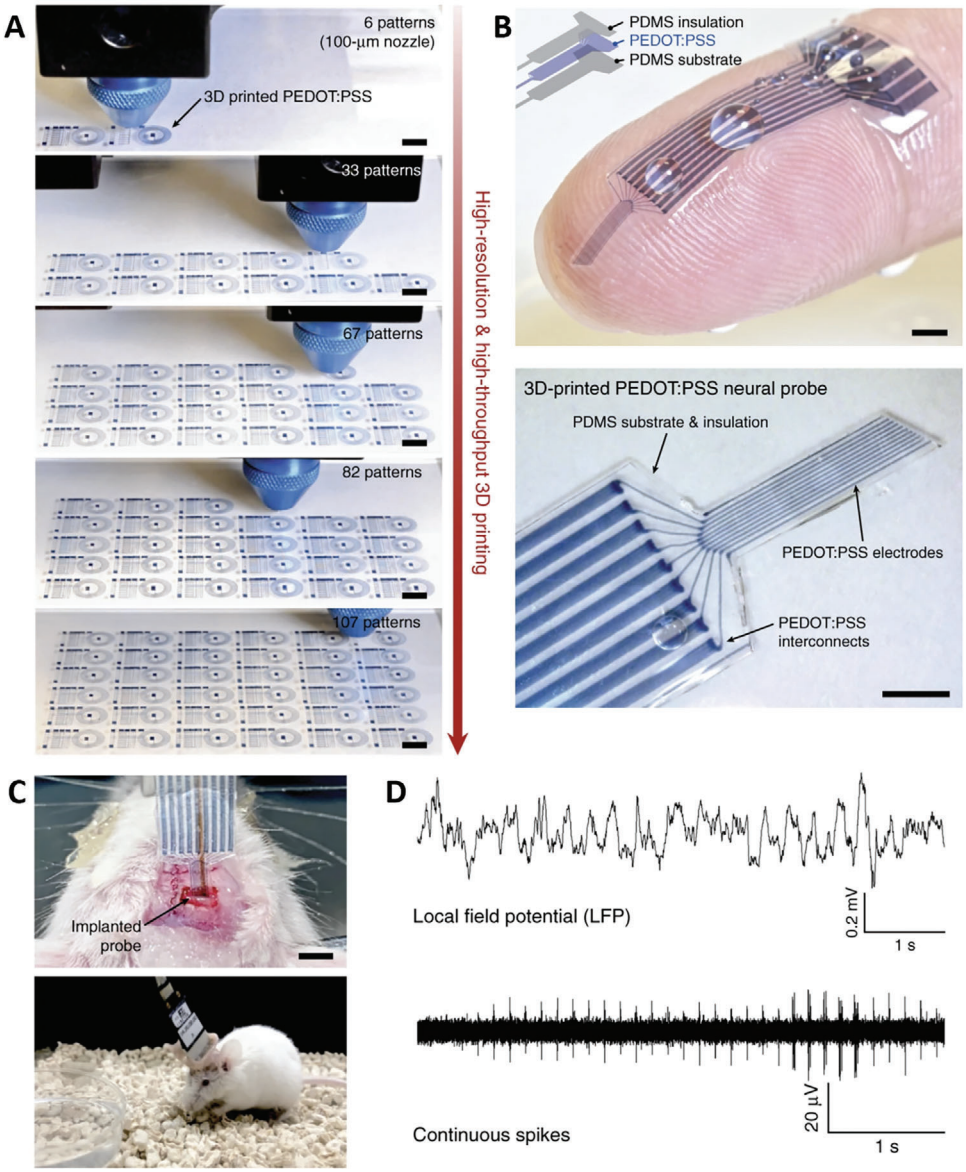

Figure 12. 3D Printing PEDOT:PSS neural electrodes. A) Lyophilized PEDOT:PSS dispersed in water/DMSO is 3D printed using a 100 um nozzle (Scale bars = 5 mm). B) PEDOT:PSS electrode active sites and interconnects are encapsulated in PDMS to form a neural interfacing electrode array (Scale bar = 1 mm). C) Electrode array is implanted in mouse dorsal hippocampus with a tethered approach (Scale bar = 2 mm). D) Representative local field potential and spike recordings from the implanted PEDOT:PSS electrode array. Reproduced with permission.[64] Copyright 2020, Springer Nature.

a study in which aqueous PEDOT:PSS was lyophilized and then redispersed in water/DSMO to create a 3D printable gel. Neural electrodes were fabricated using this 3D printing technique and tested in vivo.[64]

Finally, the same electrohydrodynamic principle of a voltage drawing a fluid out of a nozzle in a thin, continuous fiber that is employed in melt electrowriting was first discovered in electrospinning. Electrospinning also deposits thin fibers on a collector mechanism by drawing a polymer solution out of nozzle via an applied voltage potential.[65] Zhou et al. describes the development of a bicontinuous CH ink that is readily applicable to advanced fabrication methods such as spin-coating, electrospinning, soft-lithography, and 3D printing.[66] The ink was composed of two continuous phase-separated networks, an "electrical phase" consisting of PEDOT:PSS, and a "mechanical phase" consisting of hydrophilic polyurethane. The resultant composite achieves conductivities of ≈10 S cm^{-1} while maintaining a stretchability of over 400%. The viscosity of the CH ink can be tailored for each of these different fabrication methods by controlling the amount of solvent present in the ink. Furthermore, Zhou et al. demonstrated the fabrication of an all-hydrogel bioelectronic interface via selective printing of the bicontinuous CH in addition to insulating and adhesive hydrogels to produce a sutureless electrode array. This sutureless array was subsequently used to make in vivo electrophysiological recordings from rat hearts, as well as in vivo stimulation of sciatic nerve

and spinal cord, demonstrating the flexibility of this fabrication approach.

Xie et al. describe the development of aqueous PEDOT:PSS inks designed for liquid-in-liquid 3D printing of CHs.[67] The PEDOT:PSS inks are printed within oil containing PDMS surfactants terminated with amine groups (PDMS-NH_2). The PDMS-NH_2 surfactant drives the self-assembly of PEDOT:PSS colloids at the water-oil interface, trapping the CH in non-equilibrium shapes for subsequent gelation and/or cross-linking. The formation of the elastic film at the water-oil interface also allows for the tailoring of the electrical and mechanical properties of the CH ink while maintaining the printability since this fabrication approach does not require fine-tuned viscosity or immediate gelation/cross-linking to maintain shape fidelity. Xie et al. demonstrated the use of this fabrication approach to 3D print a CH-based electrochemical microfluidic device as well as a PEDOT-based NFC antenna.

5.1.3. Laser-Based Processing

Although the most prominent method for patterning CPs is through photolithography, laser-based methods have been gaining popularity due to their relative ease of application. Instead of utilizing a patterning and subsequent etching process laser-based methods aim to directly pattern CPs via photothermal ablation.[68] Laser ablation is the predominant method for laser-based patterning and has been used to successfully create well-defined areas of CP-based materials ranging from coatings to composite materials.[42,68] The primary limitation of laser patterning and micromachining methods is that the excess heat generated during the photothermal ablation can cause unwanted carbonization of the material and limits ablation to non-biological samples.[69] One promising laser-based deposition method, laser-induced forward transfer (LIFT), has been developed to enable solid-state non-contact deposition.[70] The nature of LIFT processing enables the material to be deposited without direct photothermal ablation. This method has been successfully used to pattern multiple types of CPs and has the potential to enable high-precision patterning of a wider range of sensitive CP materials.[71]

5.1.4. Post-Processing Functionalization

Perhaps the area of the electrode design space with the largest room for exploration is chemical modification of the polymer network for any application. Only a few key examples of biofunctionalization for electrode design are described in this section, but creativity is the only limiting factor when choosing a biomolecule to incorporate into the polymer matrix because of the innumerable options for realized and yet unrealized applications. The two overarching goals of chemical modification of the side chains in a polymer network of an electrode are to enhance the biocompatibility and functionality of the electrode. Biocompatibility enhancement aims to increase cell adhesion for more conformable electrode fittings with extracellular matrix proteins and to decrease the foreign body response with anti-inflammatory biomolecules. Higher cell adhesion has been achieved by the conjugation of collagen and fibrin onto carboxylic acid dopants used in the production of the CP.[72] Integration into the tissue increases long-term stability of implantation of the electrode array while also lowering the degree of foreign body response due to the intermediate layer of extracellular matrix at the surface of the electrode. A further method of decreasing the foreign body response is to modulate macrophage polarization by conjugating the polymer electrode surface with small molecules (specifically cytokines) that regulate the inflammatory response.[73] Other chemical modifications have the primary aim of enhancing the functionality of the polymer-based electrode. The incorporation of diamine-terminated PDMS as a cross-linker in organic polymers enables the process of self-healing due the low glass transition temperature of the PDMS chains. Therefore, an electrode array using a CP electrode both composed of and encapsulated by self-healing polymer networks is able to stretch and grow with underlying tissue without causing stress and damage.[74]

The advent of polymer bioelectronics has expanded the possibilities for fabrication of conformal devices that better interact with the target tissues and are designed for improved biocompatibility within the space-restricted and motile biological environment of neural interfaces. Through this wide range of fabrication approaches coupled with commensurate advances in miniaturization of electronic hardware and on-board signal processing through artificial intelligence and machine learning, fully implantable and closed-loop devices can be realized.

6. Closing the Loop with Conducting Polymers

Closing the loop in bioelectronics has been explored in research for many years. An ideal closed loop system detects specific biomarkers by continuously classifying recorded neural signals, and subsequently generating a stimulation protocol onboard an implanted integrated circuit to appropriately modulate the target neural tissue. Using closed loop feedback enables a constantly controlled system with minimal interaction by a clinician or biomedical engineer. However, the development of both effective recording and stimulation hardware that addresses a single electrode array has not yet been realised within the clinic, with the exception of devices with very low electrode counts (for example cardiac pacemakers). Historically, closed loop devices have been proposed to have Pt electrodes for stimulation and Ag/AgCl or TiN recording electrodes. This is to limit charge injection to capacitive mechanisms during stimulation but gain the sensitivity of ionically interacting materials for recording. The benefit of the mixed mode conduction from CPs enables both neural recording and stimulation from the same electrode interface. This has the added benefit of keeping the surgical footprint of the electrode for a closed-loop device as small as possible.

Some key examples of clinically relevant targets are neuromotor action potentials in a peripheral nerve of stroke patients, automated reflexes in neuroprosthesis users or sensing and quiescence of seizure in epilepsy patients. In one of the very few studies that demonstrates closed-loop functionality with CP electrodes, Zhao et al.[75] used an electrode array of PEDOT:PSS coated parylene-C shanks to explore modulation of the hippocampal-cortical communication to suppress unwanted hippocampal discharges between seizures, as seen in **Figure 13**. The low impedance recording and high charge capacity

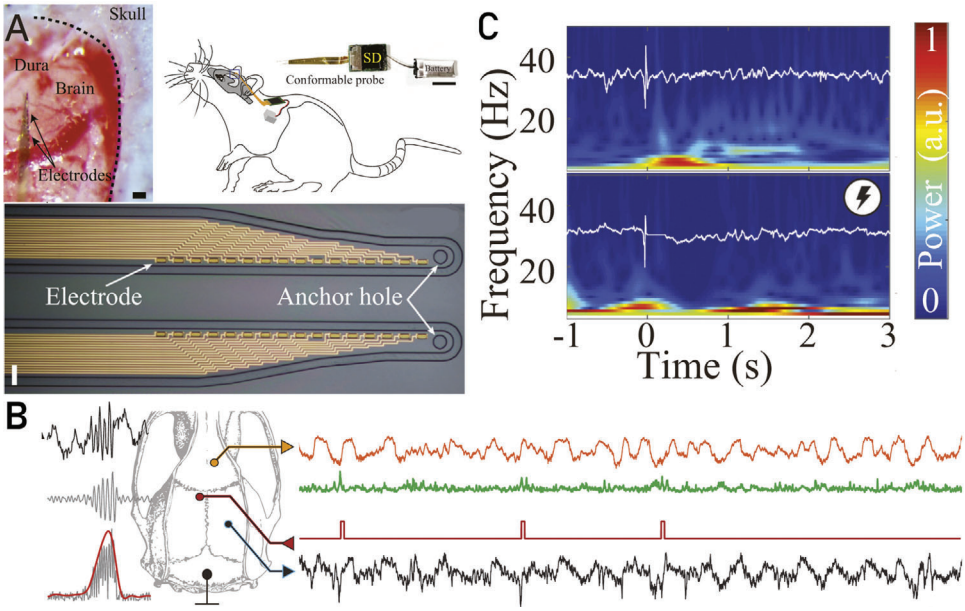

Figure 13. Suppression of Hippocampal Discharges with Closed-Loop Stimulation. A) Implantation placement in hippocampal region of rat brain, implanted with controller and battery (scale bar = 50 μm). B) Electrode array design, 16 linearly align PEDOT:PSS electrodes along a parylene-C shank (scale bar = 20 μm). C) Differentiation of initial hippocampal recording (black), processed recorded signal for triggering (green), and the corresponding triggered stimulation waveform (red). D) Time-frequency spectrogram showing IED-triggered responses in hippocampus without closed loop suppression (upper) and with closed loop suppression (lower, lightening symbol). Reproduced with permission.[75] Copyright 2021, PNAS.

stimulation capabilities of organic polymer-based electrodes enable this closed-loop functionality in CP-based electronics.

While there are limited examples of devices which close the loop in this way. There are many examples of CP-based electrodes being used separately for stimulating and recording electrodes. CP-coated and CP composite electrodes have been shown to be effective in stimulation for bionic vision, cochlear implants, deep brain stimulation, and functional electrical stimulation.[76–79] Conversely, CP-based electrodes have been used for improving the sensitivity of implanted ECoG arrays, motor control of upper limb prostheses, and brain-machine interfaces.[80–82] It is clear that with development of electronics in parallel with these electrode technologies there is a pathway for enabling closed-loop bionic devices.

This review has discussed at length the parameter space for the optimization of electrode interfaces incorporating CPs. Although this parameter space is large, the field of bioelectronics has expanded to include many experimental devices utilizing this technology. It is clear that with the novel materials being developed and tested incorporating the unique properties of CPs in conjunction with improved mechanical stability and processability of composite materials the success of closed-loop devices is closer than ever.

7. Conclusion

CP-based bioelectronics have received significant focus over the past twenty years due to their unique properties and capacity for high-performance as both stimulating and recording electrodes. The early major limitations of CP-based devices, namely robustness and manufacturability, have been overcome by the commercial introduction of processible PEDOT:PSS, and the wide array of PEDOT-based composites that have been reported in the literature. Despite this, there has been limited impact in terms of clinical translation. However, as demand rises for miniaturized bioelectronic devices, high-density electrode arrays, and closed-loop systems with recording and stimulating capacity, polymer-based bioelectronics are well positioned to give rise to a new generation of bioelectronic devices.

Acknowledgements

E.A.C. and Z.K.B. contributed equally to this work as co-first authors. The authors acknowledge funding from the Engineering and Physical Sciences Research Council (EPSRC) as part of an IRC grant on Hard-to-treat cancers [EP/S009000/1] and the Healthcare Technologies Challenge Awards (HTCA) grant. Additionally, C.A.R.C. acknowledges funding from a Rosetrees Trust Enterprise Fellowship [EF2020\100033].

Conflict of Interest

The authors declare no conflict of interest.

Keywords

conductive polymers, electrodes, recording, stimulation

Received: December 13, 2023
Revised: March 31, 2024
Published online:

[1] H. Lorach, A. Galvez, V. Spagnolo, F. Martel, S. Karakas, N. Intering, M. Vat, O. Faivre, C. Harte, S. Komi, J. Ravier, T. Collin, L. Coquoz,

I. Sakr, E. Baaklini, S. D. Hernandez-Charpak, G. Dumont, R. Buschman, N. Buse, T. Denison, I. van Nes, L. Asboth, A. Watrin, L. Struber, F. Sauter-Starace, L. Langar, V. Auboiroux, S. Carda, S. Chabardes, T. Aksenova, et al., *Nature* **2023**, *618*, 126.
[2] M. Ortiz-Catalan, J. Zbinden, J. Millenaar, D. D'Accolti, M. Controzzi, F. Clemente, L. Cappello, E. J. Earley, E. Mastinu, J. Kolankowska, M. Munoz-Novoa, S. Jönsson, C. Cipriani, P. Sassu, R. Brånemark, *Sci. Rob.* **2023**, *8*, adf7360.
[3] F. R. Willett, E. M. Kunz, C. Fan, D. T. Avansino, G. H. Wilson, E. Y. Choi, F. Kamdar, M. F. Glasser, L. R. Hochberg, S. Druckmann, K. V. Shenoy, J. M. Henderson, *Nature* **2023**, *620*, 1031.
[4] S. F. Cogan, *Annu. Rev. Biomed. Eng.* **2008**, *10*, 275.
[5] W. M. Grill, S. E. Norman, R. V. Bellamkonda, *Annu. Rev. Biomed. Eng.* **2009**, *11*, 1.
[6] D. A. Robinson, *Proc. IEEE* **1968**, *56*, 1065.
[7] C. A. R. Chapman, H. Chen, M. Stamou, J. Biener, M. M. Biener, P. J. Lein, E. Seker, *ACS Appl. Mater. Interfaces* **2015**, *7*, 7093.
[8] R. A. Green, P. B. Matteucci, C. W. D. Dodds, J. Palmer, W. F. Dueck, R. T. Hassarati, P. J. Byrnes-Preston, N. H. Lovell, G. J. Suaning, *J. Neural Eng.* **2014**, *11*, 056017.
[9] D. R. Merrill, M. Bikson, J. G. R. Jefferys, *J. Neurosci. Methods* **2005**, *141*, 171.
[10] H. Yuk, B. Lu, X. Zhao, *Chem. Soc. Rev.* **2019**, *48*, 1642.
[11] A. D. Gilmour, J. Goding, L. A. Poole-Warren, C. E. Thomson, R. A. Green, International IEEE/EMBS Conference on Neural Engineering, NER, Montpellier, France, April **2015**.
[12] J. A. Goding, A. D. Gilmour, U. A. Aregueta-Robles, E. A. Hasan, R. A. Green, *Adv. Funct. Mater.* **2018**, *28*, 1702969.
[13] R. Kim, Y. Nam, Proceedings of the Annual International Conference of the IEEE Engineering in Medicine and Biology Society, EMBS, Osaka, Japan, July **2013**.
[14] P. Yin, Y. Liu, L. Xiao, C. Zhang, *Polymers* **2021**, *13*, 2834.
[15] T. H. Le, Y. Kim, H. Yoon, *Polymers* **2017**, *9*, 150.
[16] S. G. Higgins, A. Lo Fiego, I. Patrick, A. Creamer, M. M. Stevens, *Adv. Mater. Technol.* **2020**, *5*, 2000384.
[17] R. A. Green, N. H. Lovell, G. G. Wallace, L. A. Poole-Warren, *Biomaterials* **2008**, *29*, 3393.
[18] B. D. Paulsen, K. Tybrandt, E. Stavrinidou, J. Rivnay, *Nat. Mater.* **2020**, *19*, 13.
[19] D. Khodagholy, J. N. Gelinas, T. Thesen, W. Doyle, O. Devinsky, G. G. Malliaras, G. Buzsáki, *Nat. Neurosci.* **2015**, *18*, 310.
[20] C. M. Proctor, J. Rivnay, G. G. Malliaras, *J Polym Sci B Polym Phys* **2016**, *54*, 1433.
[21] T. Nezakati, A. Seifalian, A. Tan, A. M. Seifalian, *Chem. Rev.* **2018**, *118*, 6766.
[22] A. R. Hassan, Z. Zhao, J. J. Ferrero, C. Cea, P. Jastrzebska-Perfect, J. Myers, P. Asman, N. F. Ince, G. McKhann, A. Viswanathan, S. A. Sheth, D. Khodagholy, J. N. Gelinas, *Adv. Sci.* **2022**, *9*, 2202306.
[23] M. Ganji, E. Kaestner, J. Hermiz, N. Rogers, A. Tanaka, D. Cleary, S. H. Lee, J. Snider, M. Halgren, G. R. Cosgrove, B. S. Carter, D. Barba, I. Uguz, G. G. Malliaras, S. S. Cash, V. Gilja, E. Halgren, S. A. Dayeh, *Adv. Funct. Mater.* **2018**, *28*, 1700232.
[24] A. C. Paulk, J. C. Yang, D. R. Cleary, D. J. Soper, M. Halgren, A. R. O'Donnell, S. H. Lee, M. Ganji, Y. G. Ro, H. Oh, L. Hossain, J. Lee, Y. Tchoe, N. Rogers, K. Kilic, S. B. Ryu, S. W. Lee, J. Hermiz, V. Gilja, I. Ulbert, D. Fabo, T. Thesen, W. K. Doyle, O. Devinsky, J. R. Madsen, D. L. Schomer, E. N. Eskandar, J. W. Lee, D. Maus, A. Devor, et al., *Cereb. Cortex* **2021**, *31*, 3678.
[25] S. Venkatraman, J. Hendricks, Z. A. King, A. J. Sereno, S. Richardson-Burns, D. Martin, J. M. Carmena, *IEEE Trans. Neural Syst. Rehabil. Eng.* **2011**, *19*, 307.
[26] R. A. Green, P. B. Matteucci, R. T. Hassarati, B. Giraud, C. W. D. Dodds, S. Chen, P. J. Byrnes-Preston, G. J. Suaning, L. A. Poole-Warren, N. H. Lovell, *J. Neural Eng.* **2013**, *10*, 016009.
[27] C. Boehler, Z. Aqrawe, M. Asplund, *Bioelectron. Med.* **2019**, *2*, 89.
[28] M. Bianchi, A. De Salvo, M. Asplund, S. Carli, M. Di Lauro, A. Schulze-Bonhage, T. Stieglitz, L. Fadiga, F. Biscarini, *Adv. Sci.* **2022**, *9*, 2104701.
[29] I. M. Salman, O. Z. Ameer, S. McMurray, S. F. Hassan, A. Sridhar, S. J. Lewis, Y. H. Hsieh, *Sci. Rep.* **2022**, *12*, 12242.
[30] R. Thakur, F. P. Aplin, G. Y. Fridman, *Micromachines* **2021**, *12*, 1522.
[31] M. I. Muzquiz, L. Mintch, M. R. Horn, A. Alhawwash, R. Bashirullah, M. Carr, J. H. Schild, K. Yoshida, *Sensors (Basel)* **2021**, *21*, 4521.
[32] J. Leal, S. Shaner, L. Matter, C. Böhler, M. Asplund, *Adv. Mater. Interfaces* **2023**, *10*, 2202041.
[33] S. W. Shaner, M. Islam, M. B. Kristoffersen, R. Azmi, S. Heissler, M. Ortiz-Catalan, J. G. Korvink, M. Asplund, *Biosens. Bioelectron. X* **2022**, *11*, 100143.
[34] R. Das, F. Moradi, H. Heidari, *IEEE Trans. Biomed. Circuits Syst.* **2020**, *14*, 343.
[35] R. Green, M. R. Abidian, *Adv. Mater.* **2015**, *27*, 7620.
[36] N. Yi, M. R. Abidian, *Biosynth. Polym. Med. Appl.* **2016**, 243.
[37] A. N. Dalrymple, U. A. Robles, M. Huynh, B. A. Nayagam, R. A. Green, L. A. Poole-Warren, J. B. Fallon, R. K. Shepherd, *J. Neural Eng.* **2020**, *17*, 026018.
[38] L. V. Kayser, D. J. Lipomi, *Adv. Mater.* **2019**, *31*, 1806133.
[39] J. Heck, J. Goding, R. Portillo Lara, R. Green, *Acta Biomater.* **2022**, *139*, 259.
[40] M. P. Groover, *Fundamentals of Modern Manufacturing: Materials, Processes, and Systems*, Wiley, New York **2007**, p. 1022.
[41] A. J. T. Teo, A. Mishra, I. Park, Y. J. Kim, W. T. Park, Y. J. Yoon, *ACS Biomater. Sci. Eng.* **2016**, *2*, 454.
[42] E. A. Cuttaz, C. A. R. Chapman, O. Syed, J. A. Goding, R. A. Green, *Adv. Sci.* **2021**, *8*, 2004033.
[43] F. Stauffer, M. Thielen, C. Sauter, S. Chardonnens, S. Bachmann, K. Tybrandt, C. Peters, C. Hierold, J. Vörös, *Adv. Healthcare Mater.* **2018**, *7*, 1700994.
[44] M. Gori, G. Vadalà, S. M. Giannitelli, V. Denaro, G. Di Pino, *Front. Bioeng. Biotechnol.* **2021**, *9*, 411.
[45] M. Hayashi, K. Sugimoto, A. Takasu, *Macromol. Mater. Eng.* **2019**, *304*, 1900147.
[46] K. H. Jeong, D. Park, Y. C. Lee, *J. Polym. Res.* **2017**, *24*, 112.
[47] R. A. Green, R. T. Hassarati, J. A. Goding, S. Baek, N. H. Lovell, P. J. Martens, L. A. Poole-Warren, *Macromol. Biosci.* **2012**, *12*, 494.
[48] J. Goding, A. Gilmour, P. Martens, L. Poole-Warren, R. Green, *Adv. Healthcare Mater.* **2017**, *6*, 1601177.
[49] N. A. Staples, J. A. Goding, A. D. Gilmour, K. Y. Aristovich, P. Byrnes-Preston, D. S. Holder, J. W. Morley, N. H. Lovell, D. J. Chew, R. A. Green, *Front. Neurosci.* **2018**, *11*, 748.
[50] Y. Liu, J. Liu, S. Chen, T. Lei, Y. Kim, S. Niu, H. Wang, X. Wang, A. M. Foudeh, J. B. H. Tok, Z. Bao, *Nat. Biomed. Eng.* **2019**, *3*, 58.
[51] L. Guo, M. Ma, N. Zhang, R. Langer, D. G. Anderson, *Adv. Mater.* **2014**, *26*, 1427.
[52] L. Zhang, K. S. Kumar, H. He, C. J. Cai, X. He, H. Gao, S. Yue, C. Li, R. C. S. Seet, H. Ren, J. Ouyang, *Nat. Commun.* **2020**, *11*, 4683.
[53] L. V. Kayser, M. D. Russell, D. Rodriquez, S. N. Abuhamdieh, C. Dhong, S. Khan, A. N. Stein, J. Ramírez, D. J. Lipomi, *Chem. Mater.* **2018**, *30*, 4459.
[54] X. Zheng, K. M. Woeppel, A. Y. Griffith, E. Chang, M. J. Looker, L. E. Fisher, B. J. Clapsaddle, X. T. Cui, *Adv. Healthcare Mater.* **2019**, *8*, 1801311.
[55] X. S. Zheng, A. Y. Griffith, E. Chang, M. J. Looker, L. E. Fisher, B. Clapsaddle, X. T. Cui, *Acta Biomater.* **2020**, *103*, 81.
[56] Y. Gu, J. Zhao, J. A. Johnson, *Angew. Chem., Int. Ed.* **2020**, *59*, 5022.
[57] C. Duc, G. Stoclet, J. Soulestin, C. Samuel, *ACS Appl Polym Mater* **2021**, *6*, 2366.
[58] M. Altan, *Recent Research in Polymerization*, IntechOpen, Rijeka, Croatia **2017**.
[59] P. D. Dalton, *Curr. Opin. Biomed. Eng.* **2017**, *2*, 49.

[60] K. I. Ritzau-Reid, C. D. Spicer, A. Gelmi, C. L. Grigsby, J. F. Ponder, V. Bemmer, A. Creamer, R. Vilar, A. Serio, M. M. Stevens, *Adv. Funct. Mater.* **2020**, *30*, 2003710.
[61] C. A. R. Chapman, K. Aristovich, M. Donega, C. T. Fjordbakk, T. R. Stathopoulou, J. Viscasillas, J. Avery, J. D. Perkins, D. Holder, *J. Neural Eng.* **2018**, *16*, 016001.
[62] J. R. Chan, X. Q. Huang, A. M. Song, *J. Appl. Phys.* **2006**, *99*, 023710.
[63] A. Nikoubashman, V. E. Lee, C. Sosa, R. K. Prud'homme, R. D. Priestley, A. Z. Panagiotopoulos, *ACS Nano* **2016**, *10*, 1425.
[64] H. Yuk, B. Lu, S. Lin, K. Qu, J. Xu, J. Luo, X. Zhao, *Nat. Commun.* **2020**, *11*, 1604.
[65] Y. Li, J. Zhu, H. Cheng, G. Li, H. Cho, M. Jiang, Q. Gao, X. Zhang, *Adv. Mater. Technol.* **2021**, *6*, 2100410.
[66] T. Zhou, H. Yuk, F. Hu, J. Wu, F. Tian, H. Roh, Z. Shen, G. Gu, J. Xu, B. Lu, X. Zhao, *Nat. Mater.* **2023**, *22*, 895.
[67] X. Xie, Z. Xu, X. Yu, H. Jiang, H. Li, W. Feng, *Nat. Commun.* **2023**, *14*, 4289.
[68] W. Wang, F. Qin, X. Jiang, X. Zhu, L. Hu, C. Xie, L. Sun, W. Zeng, Y. Zhou, *Org. Electron.* **2020**, *87*, 105954.
[69] S. Ravi-Kumar, B. Lies, X. Zhang, H. Lyu, H. Qin, *Polym. Int.* **2019**, *68*, 1391.
[70] M. A. Mahmood, A. C. Popescu, *Polymers* **2021**, *13*, 2034.
[71] A. Ramanavicius, A. F. Bonciu, F. Andrei, A. Palla-Papavlu, *Materials* **2023**, *16*, 1744.
[72] X. Liu, Z. Yue, M. J. Higgins, G. G. Wallace, *Biomaterials* **2011**, *32*, 7309.
[73] Y. Qian, L. Li, Y. Song, L. Dong, P. Chen, X. Li, K. Cai, O. Germershaus, L. Yang, Y. Fan, *Biomaterials* **2018**, *164*, 22.
[74] Y. Liu, J. Li, S. Song, J. Kang, Y. Tsao, S. Chen, V. Mottini, K. McConnell, W. Xu, Y. Q. Zheng, J. B.-H. Tok, P. M. George, Z. Bao, *Nat. Biotechnol.* **2020**, *38*, 1031.
[75] Z. Zhao, C. Cea, J. N. Gelinas, D. Khodagholy, *Proc. Natl. Acad. Sci. USA* **2021**, *118*, 2022659118.
[76] R. A. Green, G. J. Suaning, L. A. Poole-Warren, N. H. Lovell, 2009 4th International IEEE/EMBS Conference on Neural Engineering, NER '09, Antalya, Turkey, May **2009**.
[77] A. A. Guex, N. Vachicouras, A. E. Hight, M. C. Brown, D. J. Lee, S. P. Lacour, *J. Mater. Chem. B* **2015**, *3*, 5021.
[78] C. Bodart, N. Rossetti, J. Hagler, P. Chevreau, D. Chhin, F. Soavi, S. B. Schougaard, F. Amzica, F. Cicoira, *ACS Appl. Mater. Interfaces* **2019**, *11*, 17226.
[79] B. Ferrigno, R. Bordett, N. Duraisamy, J. Moskow, M. R. Arul, S. Rudraiah, S. P. Nukavarapu, A. T. Vella, S. G. Kumbar, *Bioact. Mater.* **2020**, *5*, 468.
[80] C. M. Frost, B. Wei, Z. Baghmanli, P. S. Cederna, M. G. Urbanchek, *Plast. Reconstr. Surg.* **2012**, *129*, 933.
[81] E. Castagnola, L. Maiolo, E. Maggiolini, A. Minotti, M. Marrani, F. Maita, A. Pecora, G. N. Angotzi, A. Ansaldo, M. Boffini, *IEEE Trans. Neural Syst. Rehabil. Eng.* **2015**, *23*, 342.
[82] H. S. Mandal, G. L. Knaack, H. Charkhkar, D. G. McHail, J. S. Kastee, T. C. Dumas, N. Peixoto, J. F. Rubinson, J. J. Pancrazio, *Acta Biomater.* **2014**, *10*, 2446.

Estelle A. Cuttaz is a research associate in the Department of Bioengineering at Imperial College London. She received her Ph.D. from Imperial College London, UK, for the development of soft and conductive elastomers for neuroprosthetic electrodes. Her research interests focus on developing soft and flexible polymeric materials and devices for applications in the field of wearable and implantable bioelectronics.

Zachary K. Bailey is a Ph.D. candidate at Imperial College London in bioengineering, in which he is investigating the improvement of spatial selectivity in stimulation of regenerative peripheral nerve interfaces. He completed his undergraduate education in mechanical engineering at the United States Air Force Academy before pursuing a Masters of Research at Imperial College London in bioengineering as a marshall scholar, sponsored by the British Government. He has continued his research as a Ph.D. candidate sponsored by the US Air Force Office of Scientific Research. He will be pursuing a medical degree after completion of his doctorate.

Christopher A. R. Chapman is a lecturer (assistant professor) in bioengineering at Queen Mary University of London in the School of Engineering and Materials Science. He leads the Continuous Advanced Recording for Cancer lab which is focused on developing bioelectronics with applications in diagnosis, monitoring, and identification of cancer. His expertise is in the field of applied bioelectronics, specifically in the fabrication and clinical translation of implanted devices for electrical stimulation and recording of the central and peripheral nervous system.

Josef A. Goding is a research associate in the Department of Bioengineering at Imperial College London and Research Director of Polymer Bionics Ltd. He received his Ph.D. from the University of New South Wales, Australia, for the development of bioactive conductive hydrogel coatings for neuroprosthetic electrodes. His research interests include soft and flexible materials for implantable and wearable bioelectronics with a focus on functional electrode materials for neural interfaces.

Rylie A. Green, FIET, is the head of bioengineering at Imperial College London. In her research, she has developed a range of innovative materials to address the limitations that hinder the development of next-generation bioelectronic devices. Her focus was in developing electrode technologies that are soft, stretchable and mediate improved electrical charge transfer with the body, including pioneering living bioelectronics. She has also developed wearable diagnostic devices and drug delivery systems for localized chemotherapy. This research has initiated collaborations with Galvani Bioelectronics, Cochlear Ltd and the US Department of Defense.